Computer-Assisted Corneal Topography

High-Resolution Graphic Presentation and Analysis of Keratoscopy

Stephen D. Klyce

Keratoscopy is a useful clinical tool for the evaluation of topographic abnormalities of the corneal surface. However, not all the detailed information presented by keratoscope photographs is assessed easily by visual inspection. A computer-based analysis system therefore was developed to assist in the clinical interpretation of keratoscope images. With this system, deviations from sphericity are displayed in graphic form to aid in the recognition of abnormalities, and surface powers are presented in tabular form. Human eyes that are emmetropic, and eyes with keratoconus and severe astigmatism were analyzed. This process provides a useful quantitative method with which to determine corneal shape, as well as a useful adjunct to the clinical evaluation and teaching of keratoscopy. In addition, such a quantitative analysis may provide the basis for the development of new techniques for the correction of visual distortion caused by corneal surface irregularities. Invest Ophthalmol Vis Sci 25:1426–1435, 1984

Corneal topography, in great part, determines visual acuity as the corneal surface is the major refractive element in the eye. Common deviations from sphericity include spontaneous, induced, and irregular astigmatism and keratoconic distortion. Whereas the optical quality of the central cornea determines visual acuity for otherwise normal eyes, recent advances in corneal refractive surgery and contact lens research could be aided by methods that depict total corneal shape. Keratoscopy is a technique by which a pattern of bright concentric circles is imaged on the cornea, so that distortions in corneal shape appear as deviations from evenly spaced concentric circles. This is a useful adjunct in the clinical diagnosis of corneal shape anomalies. However, the photographic images are not always interpreted easily nor are subtle deviations or multiple abnormalities readily apparent.

In the quest for more detailed and quantitative information from keratoscope photographs, several advances have been made. The placedo disk has been refined for more detailed analysis of corneal contours in the office.[1] Equations to assess corneal shape anomalies from keratoscope photographs have been published.[2] A series of indices derived from statistical analysis of digitized keratoscope photographs has been reported,[3] which could provide the basis for a computerized expert system to aid in diagnosis and in contact lens fitting.

In this article the above efforts are extended in the development of a system of computer-assisted procedures that provide high resolution, graphic representations of corneal topography accompanied by tabulation of quantifying data. The aims of this effort include: (1) an aid to clinical diagnosis, (2) a useful teaching tool for the interpretation of keratoscope photographs, and (3) a quantitative tool to assist in the planning and implementation of corrective procedures to restore emmetropia to patients with corneal shape abnormalities.

Portions of this work were reported at the Annual Meeting of the Association for Research in Vision and Ophthalmology, May 2, 1984, Sarasota, Florida.[4]

Materials and Methods

The Sun Contact Lens Co. Photo-keratoscope (Kyoto, Japan) was used in this study because it provides information on corneal shape over a larger surface area than the Corneascope manufactured by International Diagnostic Instruments, Ltd (Broken Arrow, OK). Corneas of human subjects and Lucite calibration spheres were photographed with Polaroid type 611 film. The originals were photographically enlarged ×5.00. Direct and automatic digitization of the original or enlarged data by video image analysis equipment was avoided for economy. Although a system that performs image analysis is commercially

From the Lions Eye Research Laboratories, LSU Eye Center, Louisiana State University Medical Center School of Medicine, New Orleans, Louisiana.

Supported in part by PHS grants EY03311 and EY02377 and by the Louisiana Lions Eye Foundation.

Submitted for publication November 8, 1983.

Reprint requests: Stephen D. Klyce, PhD, LSU Eye Center, 136 South Roman Street, New Orleans, LA 70112.

available as an attachment to the Photo-keratoscope, it is currently capable of analyzing only two corneal meridians.[5] In this study, a graphics digitizing tablet (Houston Ins, Model DT-11) was used to encode manually the final photographic enlargements of the Photo-keratoscope rings; each photograph required about 10 min of encoding by a trained technician.

Even with a carefully trained operator, the use of a digitizing tablet introduced errors. Electrical static and transmission errors produced an occasional wild point. Also, manual digitization introduced noise caused by involuntary hand tremor, as well as tracing error. These problems were largely eliminated by means of statistical procedures (*vide infra*).

A minicomputer (PDP 11/34A, Digital Equipment Corp.) running under the UNIX* Timesharing System was used to interpret the data stream from the digitizer, to develop the requisite computer programs, and to drive an incremental chart recorder (Houston Instruments Complot, Model DP-1-5). The programs were written in the portable C Programming Language.[6] (These programs are available on request for academic research purposes). Details of the derivations and implementation are provided in the *Appendix*.

The system (Photo-keratoscope, photographic enlargement, and calculations) is calibrated with six precision Lucite hemispheres over a nominal range of 6.9–8.4 mm. The radius of curvature of the hemispheres is read to within 50 μm with a convex radius gauge.

Results

Calibration

Results of calibration are shown in Figure 1; the correspondence between the physical measurement and the calculated values for the radii of curvature is linear. Importantly, this calibration validates the use of *Appendix* equation 7, in which the working distance (from Photokeratoscope face plate to the corneal image of the innermost mire) is assumed to be constant.

Repeatability of the calculated measurements was assessed by comparing means and errors of the innermost ring radii calculated from two photographs of a nominal 8.10-mm reference sphere. There was no significant difference between these measurements (8.137 ± 0.015, 8.138 ± 0.023, n = 6, $P = 0.941$).

In addition, the accuracy obtained with the outer Photo-keratoscope rings was examined without finding any systematic errors. On the basis of these measurements, the method appears to have an overall error range of less than 100 μm in the measurement of radius of curvature. For reference, the photograph and graphic analysis of an 8.4-mm calibration sphere are shown in Figure 2.

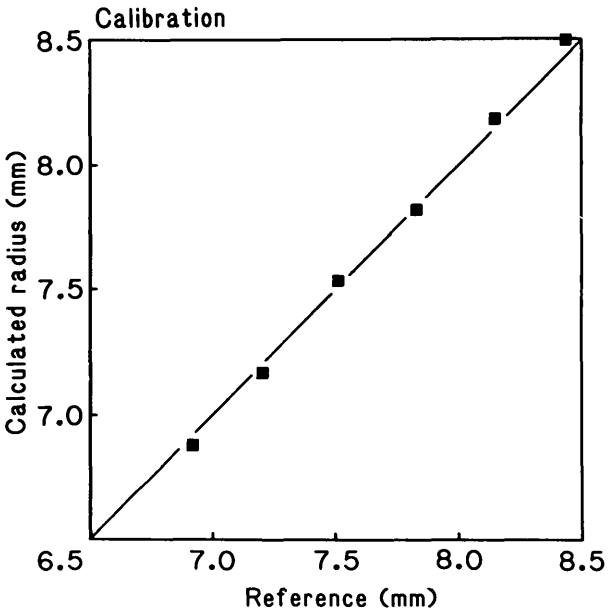

Fig. 1. System calibration. The average radius of curvature for six tracings of each of the six reference hemisphere rings is plotted against the reference measurements made with a radius gauge. The line of identity is drawn. The standard deviations of the measured values ranged from 7–30 μm, which are less than the scaled dimensions of each symbol (50 μm), and are therefore not illustrated. The correlation coefficient (from linear regression) is 0.998 ($P < 0.001$), the slope is 1.007 ± 0.025, and the intercept is 0.036 ± 0.032.

Patient Data

Results of the analysis for a normal emmetropic eye are presented in Figure 3. Beyond some minor peripheral flattening of this cornea, the difference plot shows no abnormality by comparison to a sphere.

The results of a diagnosed keratoconus case are presented in Figure 4. By comparison to the emmetropic eye shown in Figure 3, the difference plot shows severe distortion from sphericity. This distortion is recognized easily as a keratoconic cornea, with a nearly central conical apex. The diagnosis is, therefore, readily confirmed.

The results of a referred patient with postsurgical (penetrating keratoplasty) severe corneal astigmatism are shown in Figure 5. The difference plot has the mathematical shape of a saddle or a potato chip. The axis of the induced cylinder and its severity can be ascertained from the accompanying quantitative documentary report (Table 1) to serve as a guide for clinical corrective measures.

* UNIX is a trademark of Bell Laboratories.

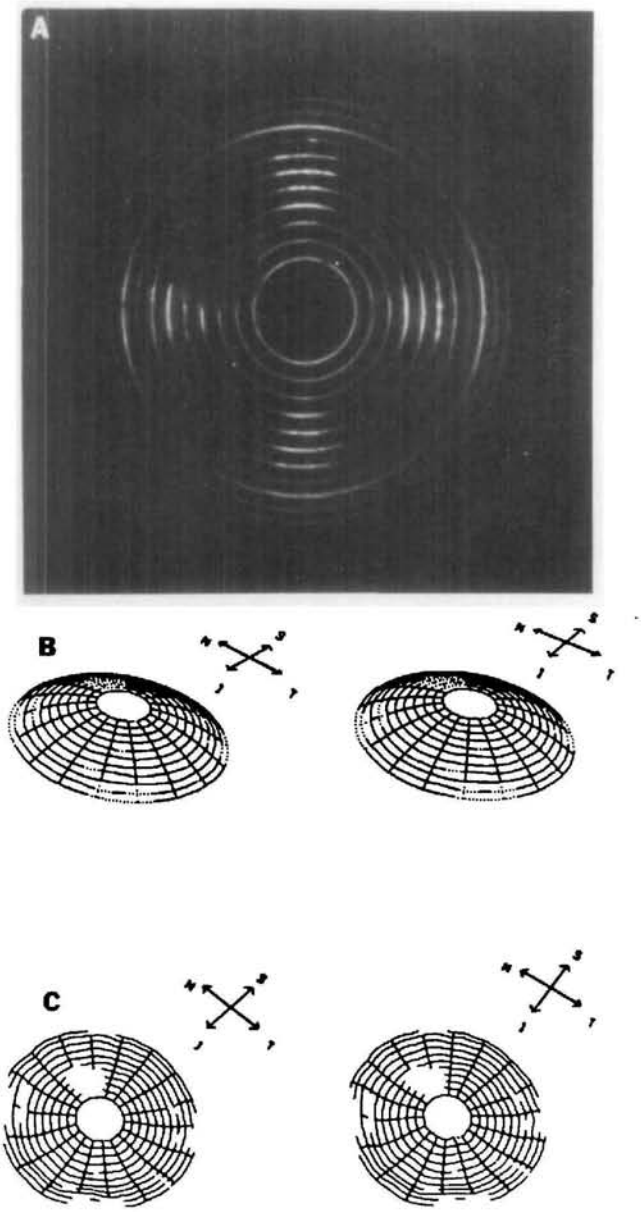

Fig. 2. Analysis of a 8.4-mm Lucite calibration surface. **A**, Photo-keratoscope photograph. **B**, Stereo pair of the calculated shape. Note that the dotted regions are areas of interpolation. **C**, Stereo pair of the surface exaggerating the differences (minimal here) between the shape shown in **B** and that of a perfect sphere. Scales are not provided as they are not useful in perspective transforms. Rather, detailed quantitative information is provided separately in tabular form (Abbreviations: S = superior; I = inferior; N = nasal; T = temporal).

As a final example, a patient with a preliminary diagnosis of severe regular astigmatism is presented in Figure 6. It is clear from the difference plot that this patient was astigmatic, but had a keratoconic cornea, which is not an unusual combination for this disorder.

Discussion

The theoretic and numeric procedures presented in the *Appendix* provide a method for the analysis of corneal topography which is more accurate than others currently available. The successive approximation method described earlier[3] and also used here for the calculation of shape and power permits errors in the radius of curvature at the innermost mire to be propagated outward to the neighboring mires; however, in this study, high resolution and accuracy were obtained by eliminating the previous assumption[3] that the central corneal radius of curvature is both constant and normal (7.8 mm) and by increasing the sample size of the data obtained for each cornea.

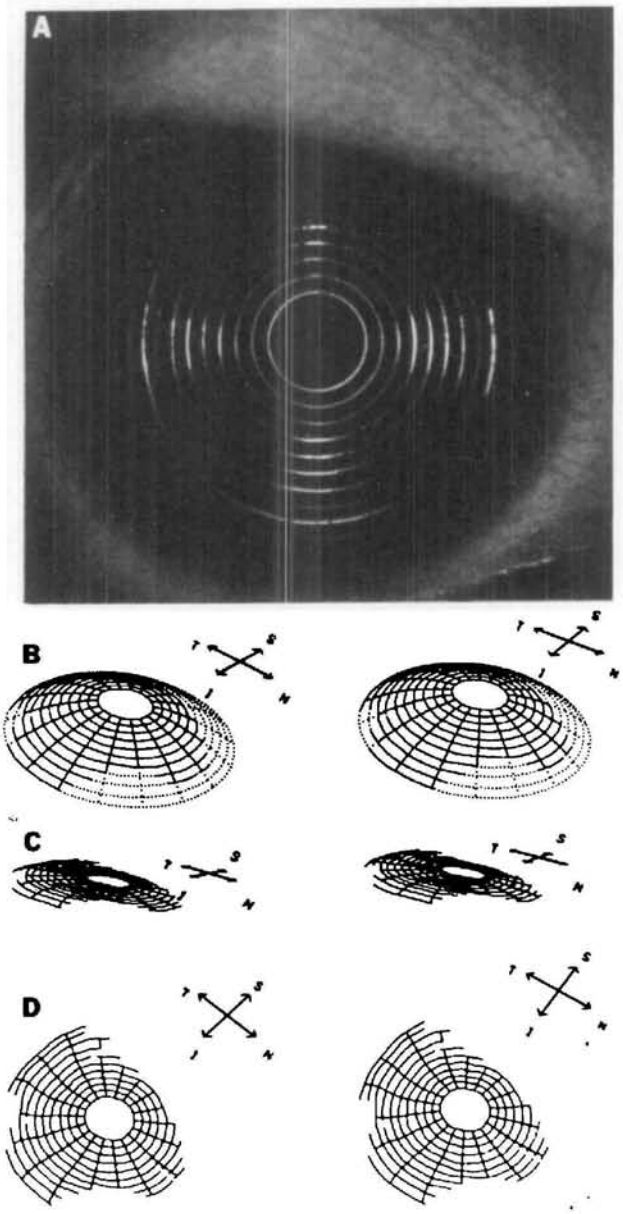

Fig. 3. Analysis of normal cornea (OD). **A**, Photo-keratoscope photograph. **B**, Stereo pair of calculated corneal shape. **C**, Stereo pair of calculated shape as it differs from the spherical. Note the difference plot shows only a slight flattening in the peripheral temporal and inferior quadrants. **D**, As in **C**, but a less tangential view.

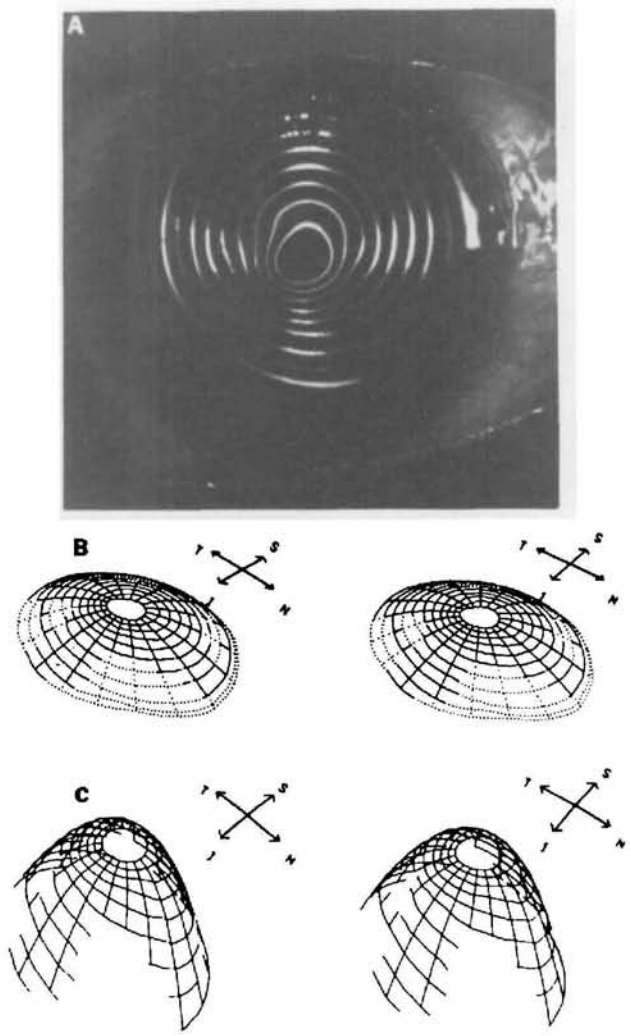

Fig. 4. Analysis of a diagnosed keratoconus cornea (OD). **A**, Photo-keratoscope photograph. **B**, Stereo pair of calculated corneal shape. **C**, Stereo pair of calculated shape as it differs from the spherical. The presence of the conical deviation is clearly illustrated.

The precision of the measurements is demonstrated by the calibration procedures, in which spheres of known radii were used as test subjects. Imperfections in the optical systems (Photo-keratoscope or enlarger) do introduce minor aspheric distortions, which could be corrected either empirically or by means of improvements in the optical system instrumentation. Such corrections may be of interest to those using the system for the creation of a statistical data base, but they are of little consequence to the clinical interpretation of corneal shape anomalies.

The graphic difference, or distortion plots, of the sample corneal shapes are novel and were developed to clearly emphasize where corneal shape deviates from that of a sphere. The sample analyses presented in this paper would not ordinarily require the sophistication of the methods used. Most corneal specialists would be able to recognize the anomalies of corneal shape by inspection of the Photo-keratoscope photographs. However, more subtle corneal distortions of early keratoconus, irregular corneal astigmatism, and the effect of surgical refractive procedures, can be recognized more easily and quantitated with the assistance of the methods developed in this work. As noted above, the Sun Contact Lens Photo-keratoscope may be purchased with a video analyzer and computer, which would obviate the need for manual digitization and intermediate photographic enlargements. However, not only is the automated system costly, but it also interpolates nearly the entire corneal surface from consideration of only two corneal meridians. This instrumentation clearly is inadequate for the evaluation of true corneal shape, except for

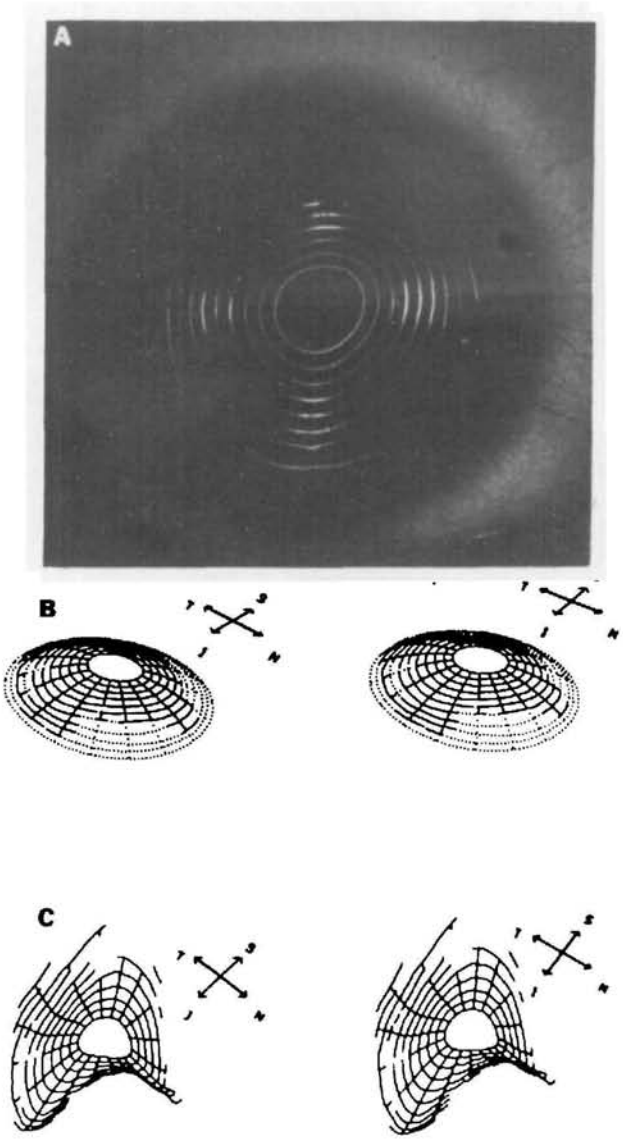

Fig. 5. Analysis of corneal shape in a case of induced astigmatism (OD). **A**, Photo-keratoscope photograph. **B**, Stereo pair of calculated corneal shape. **C**, Difference plot showing a saddle or potato chip figure characteristic of high cylinder.

Table 1. Surface powers (D) for an astigmatic cornea

	Corneal meridian (degrees)																	
Ring	*0*	*20*	*40*	*60*	*80*	*100*	*120*	*140*	*160*	*180*	*200*	*220*	*240*	*260*	*280*	*300*	*320*	*340*
0	42.97	41.06	40.10	42.10	45.31	46.97	47.56	46.30	44.59	42.77	41.83	41.74	41.42	42.36	44.78	46.72	47.08	45.70
1	43.22	41.49	40.70	42.39	45.40	47.58	48.45	46.98	44.36	42.51	42.07	42.11	40.95	41.39	43.63	45.93	47.53	46.15
2	43.83	41.98	41.47	43.17	45.68	47.90	48.99	47.27	44.22	42.42	42.24	42.10	41.13	41.08	43.20	45.74	47.70	46.67
3	44.22	42.50	42.33	43.93	46.14	48.07	49.27	47.54	44.63	42.97	42.75	41.99	41.06	41.17	43.04	46.05	47.67	46.96
4	44.46	42.98	43.29	0.00	0.00	48.54	49.43	0.00	45.00	43.67	43.45	0.00	41.51	41.22	43.33	0.00	47.88	46.99
5	44.90	43.77	0.00	0.00	0.00	0.00	0.00	0.00	45.63	44.47	44.34	0.00	42.07	41.26	43.68	0.00	47.89	46.95
6	45.04	44.66	0.00	0.00	0.00	0.00	0.00	0.00	0.00	45.17	44.57	0.00	0.00	41.95	43.81	0.00	0.00	0.00
7	44.16	0.00	0.00	0.00	0.00	0.00	0.00	0.00	0.00	45.52	44.42	0.00	0.00	42.83	44.14	0.00	0.00	0.00
8	0.00	0.00	0.00	0.00	0.00	0.00	0.00	0.00	0.00	45.55	43.87	0.00	0.00	43.16	43.97	0.00	0.00	0.00
9	0.00	0.00	0.00	0.00	0.00	0.00	0.00	0.00	0.00	45.43	0.00	0.00	0.00	0.00	0.00	0.00	0.00	0.00

To conserve space, this table is condensed by a factor of 10 from the information available from the analysis. The data resulted from the case presented in Figure 5.

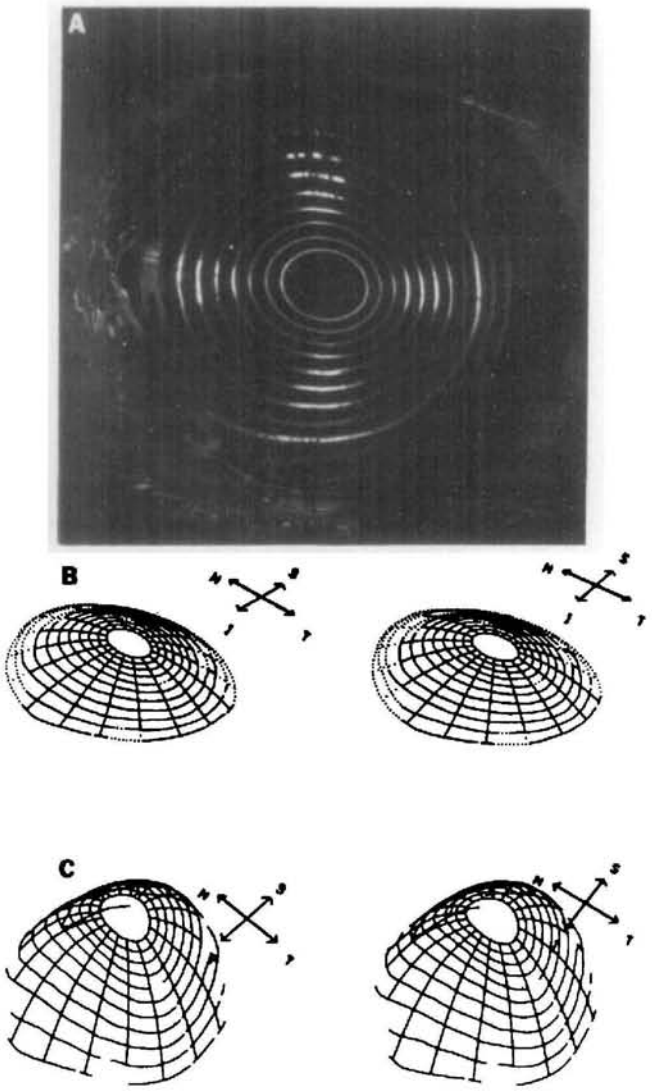

Fig. 6. Analysis of corneal shape in a case initially diagnosed as severe regular astigmatism (OS). **A**, Photo-keratoscope photograph. **B**, Stereo pair of corneal surface. **C**, Difference plot. Note the superposition of a saddle shape (astigmatism) on the cone, missed in the initial diagnosis.

corneas exhibiting radial symmetry. The current implementation uses about 7,000 points per photograph, which after passing through the smoothing routine, permits as many as 180 meridians to be analyzed. In addition, this method clearly indicates where interpolation is used to fill in regions where data are missing.

The Photo-keratoscope has advantages over the Corneascope. Foremost is its ability to cover a greater corneal surface area. In addition, the projected images of its rings are narrow by comparison, which increases the resolution of the device. However, the flash illumination is not radially uniform on the Photo-keratoscope faceplate; emphasis of the vertical and horizontal meridians can lead to data loss at intermediate meridians. Because the intensity of the illumination of the Photo-keratoscope is low during photography, compared with the Corneascope, special purpose high sensitivity films must be used to capture the image. Further degradation and data loss occur when patients with lightly pigmented irides are photographed. Yet for the purpose of accurate shape analysis, the Photo-keratoscope under ideal conditions provides more detailed information on corneal shape than the Corneascope.

The normal human corneal surface is both aspherical and variable in curvature, and its shape has a major influence on visual acuity. The older literature[6] is in general agreement on only two points in this respect for emmetropes. First, there is the notion that central corneal dioptric power is quite variable; and second, there is the belief that the cornea flattens in the periphery.[7] More recent analysis from keratoscope photographs suggests that corneas are steeper in the periphery than in the central zone.[3] Results reported here are more consistent with the earlier findings, and in keeping with lens design in which peripheral flattening is used to correct for spherical aberration.

Quite recently, a computer-based set of statistical

procedures has been described,[4] which can be used to generate indices drawn from digitized keratoscope photographs. These indices, such as image ring eccentricity, symmetry, and angularity, could be applied to form the archival basis of an "expert" computer program for the classification of corneal shapes and recognition of shape anomalies. However, these methods rely upon empirical statistical comparisons of geometric distortions of the keratoscope photograph mires, which is a transform of the actual shape of the corneal surface, while our procedure produces direct measurements of the actual corneal topography.

Computer-assisted corneal topography is a relatively young technology, but recent advances promise significant benefits to fundamental studies of corneal shape, to the teaching of keratoscope photograph interpretation, to the early diagnosis of corneal shape anomalies, and to the evaluation of new methods of corneal refractive surgery. While this paper concentrates on presenting methods and qualitative graphic depictions of corneal shapes and their deviation from sphericity, it should be noted that in the process, the means to determine accurately corneal shape and local surface power have been developed. Such data could greatly advance spectacle lens design for correction of astigmatism, for example, by adding a lens cylinder whose power and axis need not be constant. In addition, better fitting, tolerance, and optical improvement of contact lenses could be achieved by a new generation of lenses fit by considering the actual shape of the individual cornea.

Key words: cornea, keratoscopy, topography, computer analysis, human

Acknowledgments

The computer programs for this project were written in the C Programming Language on the LSU/Lions Eye Research Computer Facility, using the UNIX-operating system (courtesy of Bell Labs). The author is indebted to H. E. Kaufman for pointing out the need for this work, to J. D. Doss and R. W. Baltosser for sharing their programs and data, to C. Kelley for selecting some of the patient photographs, and to C. E. Crosson for helping to design and fabricate the hardware interface to the incremental plotter and for writing the graphics program used to produce Figures 1, A1, and A2.

Appendix

Computer Analysis of Keratoscope Photographs

Five programs were written as separate modules† to implement the goals of this project (Table A1). Currently, each component has been tested thoroughly and is fully functional. Details of the implementation are explained:

Table A1. Summary of computer-assisted corneal topography system software

Routine Name/Functions
Digitize
1. Stores key demographic patient data.
2. Stores digital coordinates for each corneal ring as entered while:
(a) approximating the coordinates of the geometric center.
(b) eliminating "wild" coordinates due to static or transmission error.
3. Converts rectangular to polar coordinates to linearize data.
4. Outputs estimated coordinates for corneal "apex" and raw digitized data.
Smooth
1. Accepts output from *digitize.*
2. Refines the estimate of the coordinates of the geometric center with statistical procedures.
3. Tags the end points of gaps (missing data) and interpolates gap coordinates.
4. Performs geometric mean of data for every 2° of arc.
5. Further smooths the data with cyclized least squares 7-point polynomial fit
6. Outputs scaled polar coordinates of smoothed data.
Keratoscope analysis program (kap)
1. Converts polar coordinate data from *smooth* to three dimensions
2. Outputs corneal elevations at incremental positions on corneal surface.
3. Generates a summary printed report of corneal dimensions.
Draw
1. Accepts data from *kap* and transforms this to two dimensions for plotting with appropriate scaling, rotation, perspective, and labeling. Outputs machine instructions to *complot.*
2. Calculates display coordinates for diagrams illustrating three dimensional portrayals of patient's corneal topography: A steroscopic surface view and a stereoscopic difference plot that exaggerates defects.
Complot
1. Accepts data from *draw* to drive the incremental plotter.
2. Waits until plotter is free.

Digitize

This program conditions the communications interface between the host computer and the digitizer to optimize host response time to the storing of data sent by the digitizer. It asks for and stores key demographic patient

† Currently, the maximum size of a compiled program on the computer used is 64,000 characters. The project was subdivided into individual functional parts each of which (invisible to the user) transmits its data directly or indirectly to the next program in sequence, which runs concurrently or is called into action by its parent process, respectively. The flexibility provided by UNIX suggests that the more powerful microcomputers could be used to implement this project. On the other hand, it should be emphasized that while UNIX and the C Programming Language are becoming widely available in portable forms, for most of the leading computer manufacturers' machines, standards for graphic input and output have not been adopted. Hence, implementation of *digitize, draw,* and *complot* on a local computer would generally require a substantial reprogramming effort.

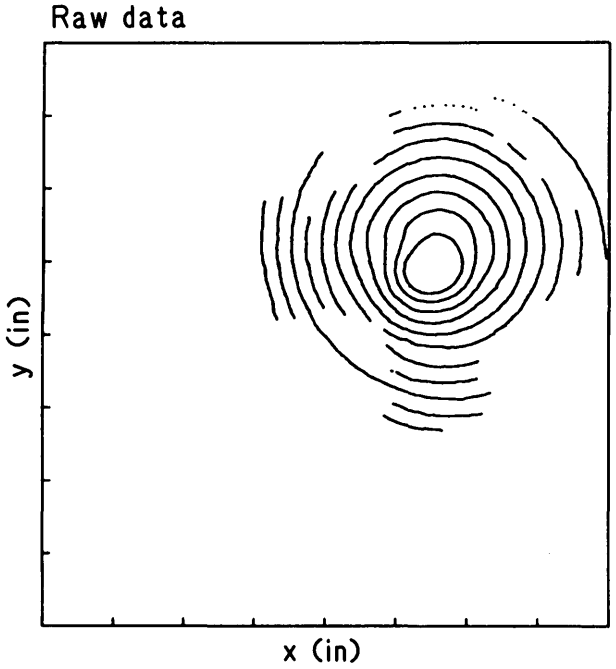

Fig. A1. Raw data collected from a Photo-keratoscope photograph with *digitize* (cf, case presented in Figure 4). Data loss is caused by lid and nose eclipse and by surface irregularities. Each division is 1 inch, the units of greatest accuracy with the current digitizer.

data to document the output and prompts the operator to trace the coordinates of each corneal ring. After the innermost ring is traced, a preliminary estimate of its geometric center is formed by calculations of the mean values of the entered vertical and horizontal coordinates. This estimate is subsequently used to convert each datum to a ring radius value, whereupon local means and standard deviations are calculated. Points that lie three standard deviations‡ away from the local mean are eliminated from the collected data. The remaining raw data are converted to polar coordinates, and these, along with the estimate for the inner ring center, are passed to the smoothing program. An example of the data from a keratoconus patient is illustrated in Figure A1. Depending upon the individual Photo-keratoscope photograph, between 5000 and 8000 points are gathered in this manner and used for the final presentations.

Smooth

This program takes its input from *digitize*, consisting of raw data coordinates and the preliminary estimate of the center of the innermost corneal ring image. Because the data are entered by manual tracing, taking the means of these coordinates for determining the center of the innermost ring image will be weighted if the data are not evenly spaced. Hence, for this ring, the polar coordinates of the raw data are integerized, missing points are filled in by linear interpolation, and duplicate points are eliminated. Following this, the unweighted estimate of the center of the innermost ring image is calculated. It is noted that the center obtained in this fashion should lie close to the visual axis for patients able to fixate.

Subsequently, for all the ring images, data missing from the raw collection are again supplied by linear interpolation between end points expressed as polar coordinates, and these interpolated data are tagged for recognition by subsequent routines. To prevent interpolated ring data from confusing the graphic display of topography in very irregularly shaped corneas, an additional algorithm is used to prevent the crossing of the interpolated coordinates of one ring over those of a more central ring.

Significant reduction of digitizing tablet operator error is achieved by averaging the raw data over each 2° of ring arc. Subsequently, a cyclized least squares 7-point polynomial averaging routine is employed for additional data smoothing.

Following these operations, *smooth* transmits the refined estimate of the innermost corneal ring center and the polar coordinates (converted to the metric system) of the smoothed actual and interpolated data to *kap*. An example of the effect of this program on the raw data is shown in Figure A2.

Keratoscope Analysis Program (*kap*)

The *kap* is the pivotal component that transforms the two-dimensional, smoothed coordinates of the keratoscope photograph to a matrix that stores the three dimensional coordinates of actual and interpolated corneal shape.

Estimation of Central Corneal Radius of Curvature. One of the shortcomings of an earlier analysis[3] concerns the normalization of calculated central corneal shape to a

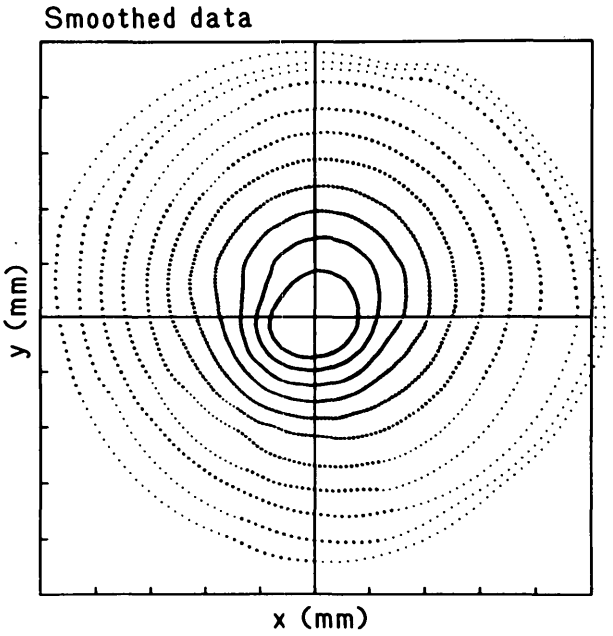

Fig. A2. Data from Figure A1 as generated by *smooth*. Each ring is represented every 2° of arc. Interpolation methods yield the finer connecting points used only for completion of the graphic forms presented. The crosshairs lie on the refined estimate of the center of the innermost shape. Each scale division is 1 mm.

‡ All statistical errors reported in this paper are expressed as standard deviations (SD).

standard 7.8 mm radius of curvature. Clearly this approach is not appropriate for ketatoconic corneas where the curvature of the central cornea may be markedly below normal, nor is this approximation adequate to estimate central corneal curvature for any cornea except one having a central power of 43.3 D. It is textbook knowledge[7] that central curvature varies considerably even among emmetropic eyes. Locking the central corneal radius of curvature to a predetermined average unduly biases the calculation of the corneal shape.

Two better approximations can be suggested for initializing the calculation. Should keratometry readings be available, these can be used as a good average estimate of central corneal curvature, although with severe corneal distortions their reliability is questionable. Where these are not available or suitable,§ the central corneal curvature can be calculated directly from keratoscope photographs with the underlying assumptions that the radius of curvature at the visual axis can be approximated from the average radius calculated from the first keratoscope corneal ring image.

The average radius of the first corneal ring image, $\bar{x}_1$ will be given by:

$$\bar{x}_1 = \sum_{i=0}^{n} x_{1,i}/n \quad (1)$$

where $x_{1,i}$ are the n radii measured with the digitizing tablet for the first corneal ring. By inspection of the Photo-keratoscope geometry (Fig. A3):

$$\tan \alpha = \bar{x}_1/wd \quad (2)$$

$$\tan (2\phi - \alpha) = (l_1 - \bar{x}_1)/wd \quad (3)$$

where wd is the manufacturer-specified working distance of the device (75 mm) and l_1 is the radius of the innermost mire on the faceplate (23 mm). Further inspection yields:

$$\phi = \theta + \alpha \quad (4)$$

$$2\phi - \alpha = 2\theta + \alpha \quad (5)$$

$$\sin \theta = \bar{x}_1/\bar{y}_0 \quad (6)$$

where $\bar{y}_0$ is the estimated elevation of the cornea at the center of the innermost ring. Combining equations 2–6 and solving for $\bar{y}_0$:

$$\bar{y}_0 = \bar{x}_1 \sin(\tan^{-1}[(l_1 - \bar{x}_1)/wd] - \tan^{-1}(\bar{x}_1/wd)) \quad (7)$$

The major error in $\bar{y}_0$ in this formulation arises from operator error in focusing the instrument, but this can be reduced considerably when attention is directed at focusing the Photo-keratoscope in a manner that places the image of the innermost mire midway in the depth of field.

In this paper, equation 7 is used exclusively to estimate the curvature at the visual axis, and the associated error is evaluated.

Calculation of Corneal Shape. As pointed out earlier,[3] an exact analytical solution to calculate corneal topography coordinates from keratoscope photographs is currently incogitable. Hence, a numerical procedure is used to obtain data from photographs made with the Photo-keratoscope.

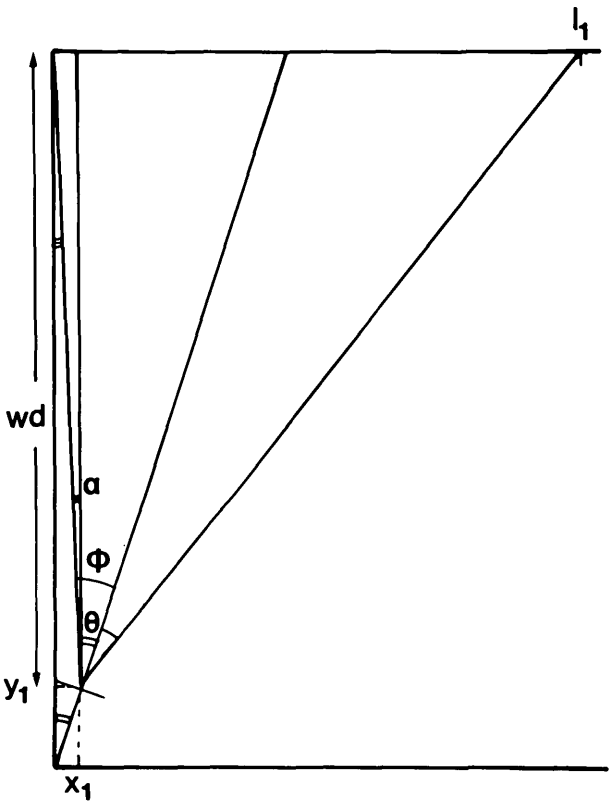

Fig. A3. Method for estimating central corneal radius of curvature. The working distance (wd = 75 mm) for the Photo-keratoscope provides a measurement of the distance between the instrument faceplate and the image of the innermost ring. The radius of the innermost ring (l_1 = 23 mm) on the faceplate is known, and the smoothed values of the radii, x_1, of the innermost ring image are sufficient to calculate the elevations, y_1. The average value of y_1 is referred to as $\bar{y}_0$ in the text, and is used as the central corneal elevation in the subsequent calculations of all ring image coordinates.

A preliminary estimate of corneal elevation y_i at ring, i, can be obtained from[2] (cf, Fig. A4):

$$y_i = y_{i-1} - \frac{(x_{i-1} - x_i)\cdot(\cos t_{i-1} - \cos t_i)}{\sin t_{i-1} - \sin t_i} \quad (8)$$

where y_i, x_i are the coordinates of elevation and ring radii, respectively, and t_i (initialized to A/2) are the angles formed by the tangents to the corneal surface and the horizontal). Improvements to y_i are obtained by iteration of equation 8 and:

$$d_0 = wd + \bar{y}_0 \quad (9)$$

$$r_i^2 = (l_i - x_i)^2 + (d_0 - y_i)^2 \quad (10)$$

$$r_r^2 = (d_0 - y_i)^2 + x_i^2 \quad (11)$$

$$A' = \cos^{-1}[(l_i^2 - r_r^2 - r_i^2)/(-2r_r^2\, r_i^2)] \quad (12)$$

$$t_i = \pi/2 - A'/2 - \tan^{-1}[(d_0 - y_i)/(l_i - x_i)] \quad (13)$$

§ The current generation of keratometers approximate surface power over a 3–4 mm meridional arc on the corneal surface. Hence, this resolution may not be appropriate in the current context.

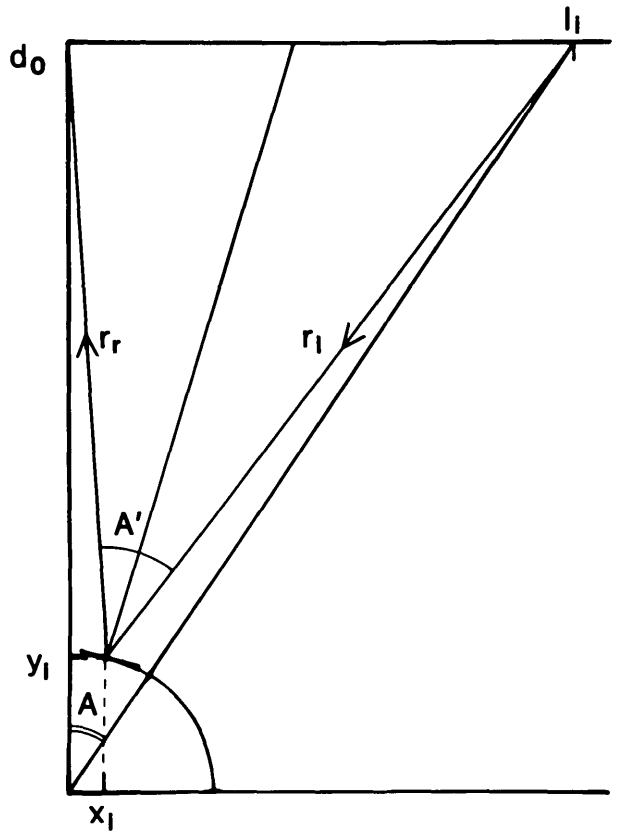

Fig. A4. Method used to calculate elevations, y_i, at each ring image locus, x_i. This is similar to an earlier approach,[3] with some alterations reflecting geometric differences between the two keratoscopes used. Importantly, d_0 (the sum of the working distance and the average central elevation, $\bar{y}_0$, for a given cornea) defines the origin for the elevation array. Angle t, (not shown) is the angle formed by the tangent to the corneal surface and the horizontal line at y_i.

until y_i changes by less than 0.00001% by comparison with the previous iteration.

Equations 8–13 differ principally from earlier work[3] in that apical corneal radius of curvature is not set to a predetermined constant, and the geometry of the keratoscope used in the work necessitates rederivation.

Calculation of Corneal Surface Powers. To compare corneal powers to keratometry readings (cf, reference 8), one can define a parameter, r_{cl}, the local radius of curvature at points along a corneal meridian. Doing so neglects chromatic and spherical lens aberrations, as well as deviations along the corneal surface parallels described by keratoscope rings. Nevertheless, with these approximations, at least two methods can be used to estimate corneal power from corneal meridia: tangent analysis and arc analysis.

Tangent analysis: Adapting earlier work[3] to Photo-keratoscope geometry, the following relationship can be devised relating the radius of a corneal keratoscope ring, x_i, and the tangent angle, t_i (cf, equation 13):

$$r_{cl} = x_i/\cos(\pi/2 - t_i) \qquad (14)$$

Arc analysis: Alternatively, the radius of curvature of the arc formed by three consecutive rings along a corneal meridian can be defined by (cf, Fig. A5):

$$r_{cl}^2 = (x_0 - h)^2 + (y_0 - k)^2$$
$$r_{cl}^2 = (x_1 - h)^2 + (y_1 - k)^2$$
$$r_{cl}^2 = (x_2 - h)^2 + (y_2 - k)^2 \qquad (15)$$

in which x's and y's are the coordinates of three adjacent rings on a single meridian, and h and k are the distances the center of the arc is displaced from the origin of the meridian profile. Equation 15 is solved for r_{cl} with:

$$k = [(x_2 - x_0)(x_0 - x_1)(x_1 - x_2) + (y_0^2 - y_1^2)(x_1 - x_2) + (y_2^2 - y_1^2)(x_0 - x_1)]/[2\langle(y_0 - y_1)(x_1 - x_2) + (y_2 - y_1)(x_0 - x_1)\rangle] \qquad (16a)$$

$$h = [x_0 + x_1 - (y_0 + y_1 - 2k)(y_0 - y_1)/(x_0 - x_1)]/2 \qquad (16b)$$

and back-substitution of h and k into any one of the eqns 15, eg:

$$r_{cl} = |\sqrt{(x_0 - h)^2 + (y_0 - k)^2}| \qquad (16c)$$

The local power K_l can then be obtained from:

$$K_l = 0.3375/r_{cl} \qquad (17)$$

in which the numerator is the gradient in refractive index between air and the eye, and r_{cl} is expressed in meters.

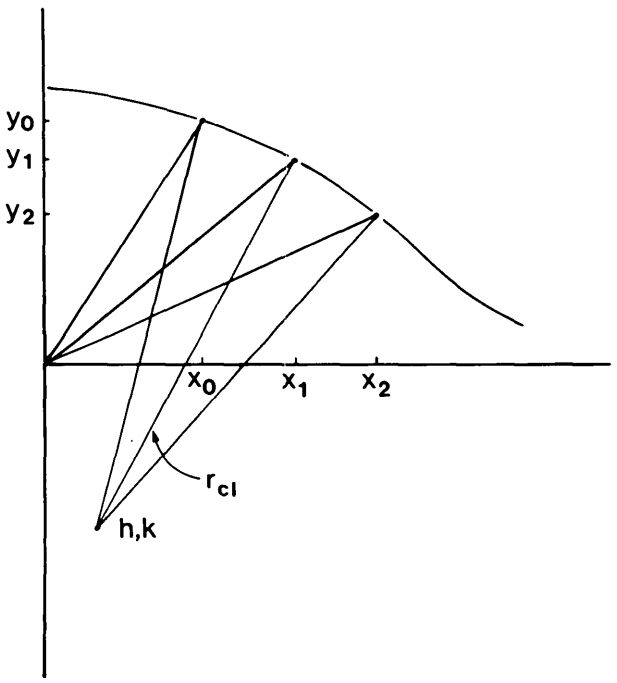

Fig. A5. Procedure for determining a local corneal radius of curvature along a corneal meridian using arc analysis. Note that the vectors intersecting at the origin will be identical to the local radius of curvature, r_{cl}, only for a perfect sphere. The parameters h and k are the coordinates for the center of the circle defined by the three points indicated.

Because the latter method has an advantage over tangent analysis for further smoothing of the reported data, equations 16–17 were used to generate report tables of corneal refractive power as a function of position to accompany the computer graphical presentation. A condensed example of such a report is shown in Table 1.

Draw

The program *draw* accepts the polar coordinates produced by kap placing these canonical data into a three dimensional matrix to depict graphic representations of the corneal surface. Rotation, perspective, and space transforms were adapted from published methods.[8] The most diagnostically useful two-dimensional graphic representations of these data were found to be stereoscopic views of actual corneal topography and of the difference between actual corneal topography and a perfect sphere. The latter difference plot was constructed by amplifying spherical deviations of individual corneal shapes. In such presentations, perfect spheres transform to flat or planar projections, while shape anomalies, such as cones and cylinders, are emphasized. Examples of this procedure are shown in the results. Importantly, *draw* was made to differentiate between actual and interpolated data so that the representations clearly indicate or exclude data not actually present in the original keratoscope photographs.

Complot

This program accepts graphic instructions from *draw*, translating these to machine instructions to drive the Complot incremental plotter. To prevent conflicts in a time sharing resource scheme, it checks current processes in operation, and waits to plot its results if a concurrent process is using the resource.

Early in the course of this project, two additional computer programs were planned. One named *diagnose* was to have looked at the data for shape anomalies such as keratoconus and astigmatism. The second, named *learn*, was to have maintained a data base containing patient histories, physician diagnoses, and diagnoses provided by *diagnose*. Such an expert system is within the realm of current technology. However, these two components were set aside when it became clear that accurate diagnoses were easily made by inspection of the graphic and tabular presentations.

References

1. Rowsey JJ, Reynolds AE, and Brown R: Corneal topography. Corneascope. Arch Ophthalmol 99:1093, 1981.
2. Doss JD, Hutson RL, Rowsey JJ, and Brown R: Method for calculation of corneal profile and power distribution. Arch Ophthalmol 99:1261, 1981.
3. Cohen KL, Tripoli NK, Pellom AC, Kupper LL, and Fryczkowski AM: A new photogrammetric method for quantifying corneal topography. Invest Ophthalmol Vis Sci 25:323, 1984.
4. Klyce SD: Computer-assisted analysis of human corneal topography. ARVO Abstracts. Invest Ophthalmol Vis Sci 25(Suppl):167, 1984.
5. Itoi M: An automated contact lens design system. J Japan Contact Lens Soc 21:271, 1979.
6. Kernighan B and Ritchie D. The C Programming Language. Englewood Cliffs, Prentice-Hall, 1978.
7. Mandell R, *locus citare*: System of Ophthalmology Vol V, Ophthalmic Optics and Refraction, Duke-Elder S and Abrams D, editors. St. Louis, CV Mosby, 1970, p. 130.
8. Girard LJ, Sampson WG, and Soper JW: Keratometry. *In* Corneal Contact Lenses, Girard LJ, Soper JW, and Sampson WG, editors. St. Louis, CV Mosby, 1964, pp. 81–106.
9. Newman WM and Sproull RF: Principles of Interactive Computer Graphics, second edition. New York, McGraw-Hill, 1979.